



Effect of hydrophobic core packing on sidechain dynamics

Eric C. Johnson^{a,b} & Tracy M. Handel^{b,*}

^a*Department of Physics, University of California, Berkeley, CA 94720, U.S.A.*

^b*Department of Molecular and Cell Biology, 229 Stanley Hall, University of California, Berkeley, CA 94720, U.S.A.*

Received 11 June 1999; Accepted 26 July 1999

Key words: CH₂D relaxation, order parameters, protein design, sidechain dynamics, ubiquitin

Abstract

The effect of hydrophobic core packing on sidechain dynamics was analyzed by comparing the dynamics of wild-type (WT) ubiquitin to those of a variant which has seven core mutations. This variant, 1D7, was designed to resemble WT by having a well-packed core of similar volume, and we find that its overall level of dynamics is only subtly different from WT. However, the mutations caused a redistribution in the positions of core residues that are dynamic. This correlates with the tendency of these residues to populate unfavorable rotamers, suggesting that strain from poor sidechain conformations may promote increased flexibility as a mechanism to relieve unfavorable steric interactions. The results demonstrate that even when core volume is conserved, different packing arrangements in mutants can alter dynamic behavior.

Introduction

A static three-dimensional structure represents only a partial picture of a protein. It is now well accepted that protein dynamics play an important role in function, binding specificity, binding affinity and thermodynamic stability. In some cases, large scale motions in proteins, observed from variations in crystal structures of the same protein (Faber and Matthews, 1990) or differences between the crystal structures of free and ligand bound proteins (Zanotti et al., 1993), show an obvious role for dynamics in the accessibility and release of substrates from active sites. However, for binding specificity and affinity of protein–ligand complexes, or for the stability of globular proteins, the role of dynamics may be more complicated to understand, even qualitatively. This is because these properties are determined by a balance between stabilizing and destabilizing interactions which may be modulated by motion, or compensated by changes in conformational entropy.

A variety of experimental methods have been used to study motions of proteins, including NMR relaxation (Palmer, 1997; Kay, 1998), molecular dynamics (Chatfield et al., 1998; Lienin et al., 1998; Wong and Daggett, 1998), normal mode calculations (Miller and Agard, 1999), and X-ray crystallography using multiple conformation refinement (Rader and Agard, 1997). Measurements of backbone dynamics by ¹⁵N relaxation experiments are now routine, generally showing highly restricted motions over regions of secondary structure and larger motions in loops. More recently, NMR experiments have also been developed to measure the dynamics of sidechain methyl groups by monitoring either ¹³C (Wand et al., 1996) or ²H (Kay et al., 1996) relaxation. These results indicate that sidechains have a large range of flexibility compared to the backbone, even in regions of the protein where the backbone is rigid. Furthermore, studies of the effects of ligand binding on backbone (Akke et al., 1993; Cheng et al., 1994; Farrow et al., 1994; Stivers et al., 1996; Hodsdon and Cistola, 1997; Olejniczak et al., 1997) and sidechain (Constantine et al., 1998; Gagne et al., 1998; Kay et al., 1998) flexibility have shown

*To whom correspondence should be addressed. E-mail: handel@paradise1.berkeley.edu

the very important result that dynamics affects both binding affinity and binding specificity.

In addition to these observations, it is important to understand what energetic interactions control dynamics and therefore affect the specificity and stability of proteins and protein complexes. Interactions which contribute to fold specificity and stability have been an area of intense interest in protein design. This is because early designs lacked structural specificity as evidenced by poor dispersion in NMR spectra, binding of the hydrophobic dye 8-anilino-1-naphthalenesulfonic acid (ANS), and usually low stability (Hecht et al., 1990; Kamtekar et al., 1993; Quinn et al., 1994; Yan and Erickson, 1994). However, the recent use of computational methods to design proteins has reversed this trend with successful core (Hurley et al., 1992; Desjarlais and Handel, 1995; Dahiyat and Mayo, 1996; Kono et al., 1998), metal binding (Pinto et al., 1997; Wisz et al., 1998) and de novo designs (Dahiyat and Mayo, 1997), some having stabilities of thermophilic proteins (Malakauskas and Mayo, 1998). Nevertheless, a quantitative understanding of the interactions contributing to the biophysical properties of proteins remains incomplete. In particular, there have been few studies which directly address how these interactions affect dynamics. Addressing this question will be an important step if we ever hope to achieve the goal of rational design of function and protein–ligand interactions.

We have focused on understanding the role of core packing on the properties of designed proteins. To this end we developed the core packing program ROC (Repacking Of Cores) which uses a genetic algorithm as a search method and a van der Waals potential as a scoring function to redesign protein cores. The program was tested by designing a number of core variants of the proteins 434 cro (Desjarlais and Handel, 1995) and ubiquitin (Lazar et al., 1997). To further evaluate the utility of the program, we solved the structure and investigated the dynamics of one ubiquitin variant, 1D7, which has 7 of its 14 core residues mutated and is destabilized by $2.0 \text{ kcal mol}^{-1}$ relative to WT (Johnson et al., 1999). We showed that the protein structure was well predicted and has only subtle differences from WT in its overall dynamic character. Here we examine in greater detail the sidechain dynamics of WT and 1D7, determined by ^2H methyl relaxation. Despite the small differences, we observe interesting correlations between the presence of sidechain strain and increased dynamics of core sidechains. To our knowledge, this is the first report of the effect of mutations on sidechain dynamics measured by NMR.

Materials and methods

Sample preparation

Fractionally deuterated $^2\text{H}/^{13}\text{C}/^{15}\text{N}$ samples of 1D7 and WT ubiquitin were prepared as previously described (Lazar et al., 1997; Johnson et al., 1999). Briefly, protein was expressed in a BL21/pLysS strain of *E. coli*, in media containing 60% D_2O and ^{13}C glucose and ^{15}N ammonium sulfate as the sole carbon and nitrogen sources. Protein was purified from the cell supernatant by ion exchange chromatography on a Fast Flow SP Sepharose column (Pharmacia), followed by size exclusion on a Superdex 75 sizing column (Pharmacia), and finally reversed-phase HPLC using a Vydac C8 column. The protein was refolded by resuspending lyophilized protein in 6 M GuHCl and dialyzing into water. The refolded protein was lyophilized a second time and resuspended in 25 mM sodium acetate, 25 mM sodium phosphate, pH 5.8. Protein concentrations were approximately 2 mM.

NMR spectroscopy

Measurements of $T1(I_zC_zD_z)$, $T1\rho(I_zC_zD_y)$, and $T1(I_zC_z)$ relaxation rates for CH_2D methyl groups were carried out on Bruker DMX600 and DRX500 spectrometers at 30°C , using the methodology of Kay and co-workers (Kay et al., 1996). For each rate, 10 experiments with various delays were recorded, one in duplicate at the end of the series to ensure that no change in sample or hardware had occurred. For measurement of $T1(I_zC_zD_z)$ and $T1(I_zC_z)$ values, delays ranged from 0.05 to 78 ms and 0.05 to 300 ms, respectively. For the $T1\rho(I_zC_zD_y)$ relaxation times, experiments were recorded with delays from 0.2 to 15.5 ms. Data were processed by apodizing with a sine bell, zero-filling once and Fourier transforming in both dimensions. For a few peaks which were partially overlapped in the ^{13}C dimension when processed by Fourier transformation, sufficient resolution for analysis was obtained by processing the indirect dimension using a maximum entropy algorithm (Hoch and Stern, 1996). Measured relaxation rates for resolved peaks were the same within error when data was processed via Fourier transform or maximum entropy (data not shown).

Data analysis

$T1(I_zC_zD_z)$, $T1\rho(I_zC_zD_y)$, and $T1(I_zC_z)$ relaxation rates were determined by least squares fitting of the peak heights to an exponential decay. Uncertainties

in the relaxation parameters were derived from the uncertainties in the fits. Motional parameters were determined by minimizing the sum of the squared residuals between the experimental relaxation rates and those calculated from the fitted parameters, using the simple model free formalism (Lipari and Szabo, 1982; Kay et al., 1996). Errors in the fitted parameters were estimated by the variation in these parameters using a Monte Carlo sampling of the relaxation rates over the range of their uncertainties. Methyl order parameters are presented as S_{axis}^2 , which is related to the generalized order parameter S^2 by $S_{\text{axis}}^2 = S^2/0.111$. This corresponds to the order parameter of the methyl symmetry axis assuming a tetrahedral methyl geometry and that the three equivalent methyl hydrogens are free to rotate.

Results

Sidechain dynamics were investigated for both WT and 1D7 by measuring the ^2H T1 and T1 ρ relaxation rates of CH_2D methyls at both 500 and 600 MHz (Kay et al., 1996). Generalized order parameters (S^2) and internal effective correlation times (τ_e) were determined by fitting the relaxation rates to the simple Lipari–Szabo model free formalism (Lipari and Szabo, 1982). Sidechain order parameters were determined for 46 methyls in 1D7 and 42 methyls in WT. In 1D7, no data were obtained for 66T γ and 70V γ 1 because of complete overlap of the crosspeaks. Likewise, in WT, data were not obtained for 8L δ 2, 26V γ 1, 43L δ 2, 66T γ , 69L δ 1, 69L δ 2, 70V γ 1, and 71L δ 2 because of spectral overlap. Furthermore, relaxation rates for 5V γ 2 and 17V γ 1 in WT were determined only at 600 MHz because of partial resonance overlap.

Motional parameters from the model free analysis are shown in Table 1, along with the fractional solvent accessible surface areas for methyl groups. Our WT order parameters are very similar to those determined by Wand and co-workers using the same method (Lee et al., 1999). We observe the same general trend as in other sidechain dynamics studies: lower order parameters for methyls further away from the backbone, and a larger dynamic range for sidechain methyl order parameters compared to backbone NH groups over the ordered regions of the protein (Kay et al., 1996, 1998; Wand et al., 1996; Constantine et al., 1998; Gagne et al., 1998; Yang et al., 1998; Mittermaier et al., 1999). In general we see that backbone flexibility is not a prerequisite for sidechain flexibility. We obtained

the following average values of S_{axis}^2 from our measurements of 1D7 and WT: Ala β 0.83 ± 0.06 , Thr γ 0.72 ± 0.14 , Val γ 0.67 ± 0.19 , Ile γ 2 0.73 ± 0.12 , Ile δ 0.44 ± 0.19 , and Leu δ 0.45 ± 0.18 (excluding Leu 73 in the disordered C-terminus; Met is not included since ubiquitin has only one). These compare surprisingly well to the averages obtained from a database of eight proteins: Ala β 0.81 ± 0.10 , Thr γ 0.72 ± 0.14 , Val γ 0.63 ± 0.18 , Ile γ 2 0.71 ± 0.11 , Ile δ 0.47 ± 0.20 , Leu δ 0.47 ± 0.20 , and Met ϵ 0.22 ± 0.12 (Mittermaier et al., 1999). The differences of the measured order parameters from the average values from the database for each methyl type ($S_{\text{axis}}^2 - \langle S_{\text{axis}}^2 \rangle$) are mapped onto the backbone structure in Figure 1 and plotted in Figures 2 and 3. The methyl carbons in Figure 1 are colored according to the difference of their order parameters from the average. Ala β methyl order parameters are not displayed because they are considered to be probes of backbone motion, consistently having high values and a weak but nevertheless statistically significant correlation with NH order parameters (Mittermaier et al., 1999).

Dynamics of surface residues

We observe only a weak anti-correlation between methyl order parameter and fractional solvent accessible surface area of methyl groups. The linear correlation coefficient, $r = -0.50$, has a probability, $p = 3.3 \times 10^{-6}$ of being the result of uncorrelated data. A correlation is generally considered statistically significant if $p < 0.05$ (Bevington, 1969). However, it is clear from Figure 1 that surface residues generally have lower order parameters, relative to average, than core residues. Furthermore, the data indicate that there is little difference between 1D7 and WT in the flexibility of surface residues (Figures 1 and 2). This provides a very sensitive indication that repacking the core of 1D7 has not perturbed the rest of the structure relative to WT to any significant extent. The largest differences in surface order parameters are for T7 and L8 methyls, which are higher in 1D7 than in WT, and for the δ methyl of I36 where the trend is reversed. One surface residue with significantly higher than average order parameters in both 1D7 and WT is M1. This sidechain is partially buried and the methyl is packed against the core. Two additional methyls that are pointing towards the solvent, yet have high order parameters, are T22 and T55. In both of these cases, the sidechains are oriented in a way that favors hydrogen bonds between the sidechain oxygen and the backbone amides of residues 25 and 58, respectively. The restricted mo-

Table 1. ^2H relaxation parameters and solvent-accessible surface area for 1D7 and WT

1D7				WT					
Residue		S_{axis}^2	τ_e (ps)	Accessibility (%)	Residue		S_{axis}^2	τ_e (ps)	Accessibility (%)
1M	ϵ	0.54 ± 0.03	9.4 ± 1.2	3.2 ± 3.1	1M	ϵ	0.60 ± 0.03	7.0 ± 2.1	0.7 ± 0.6
3V	γ_1	0.71 ± 0.03	81.0 ± 1.9	1.3 ± 1.1	3I	γ_2	0.80 ± 0.03	44.2 ± 1.8	0.0 ± 0.0
3V	γ_2	0.75 ± 0.03	78.7 ± 1.9	3.3 ± 1.9	3I	δ_1	0.63 ± 0.02	16.1 ± 1.4	0.4 ± 0.6
5L	δ_1	0.53 ± 0.03	31.2 ± 1.8	0.3 ± 0.5	5V	γ_1	0.75 ± 0.03	26.1 ± 1.8	0.8 ± 0.8
5L	δ_2	0.56 ± 0.04	55.1 ± 2.1	3.1 ± 2.8	5V	γ_2	0.74 ± 0.03	41.7 ± 1.6	1.6 ± 1.0
7T	γ_2	0.80 ± 0.04	46.6 ± 2.0	10.4 ± 6.5	7T	γ_2	0.69 ± 0.03	49.6 ± 1.7	14.3 ± 6.9
8L	δ_1	0.31 ± 0.02	51.6 ± 1.2	52.9 ± 9.7	8L	δ_1	0.19 ± 0.01	49.2 ± 0.6	40.8 ± 17.6
8L	δ_2	0.28 ± 0.01	50.8 ± 0.7	30.9 ± 8.0	8L	δ_2	n.d.	n.d.	63.2 ± 31.8
9T	γ_2	0.66 ± 0.03	35.0 ± 1.6	86.9 ± 5.1	9T	γ_2	0.62 ± 0.03	38.8 ± 2.0	74.2 ± 24.5
12T	γ_2	0.66 ± 0.04	48.6 ± 1.7	35.1 ± 8.7	12T	γ_2	0.72 ± 0.04	42.5 ± 2.1	26.0 ± 8.8
13V	γ_1	0.47 ± 0.02	65.1 ± 1.2	27.6 ± 11.9	13I	γ_2	0.51 ± 0.02	43.6 ± 1.4	22.2 ± 7.9
13V	γ_2	0.38 ± 0.02	81.8 ± 1.0	6.4 ± 3.5	13I	δ_1	0.46 ± 0.02	27.3 ± 1.1	5.3 ± 2.9
14T	γ_2	0.49 ± 0.02	64.9 ± 1.5	29.6 ± 8.6	14T	γ_2	0.59 ± 0.03	58.4 ± 1.9	29.9 ± 10.3
15I	γ_2	0.62 ± 0.02	56.0 ± 1.2	14.7 ± 4.7	15L	δ_1	0.47 ± 0.04	46.8 ± 2.7	0.9 ± 1.5
15I	δ_1	0.26 ± 0.02	38.3 ± 1.0	3.3 ± 4.0	15L	δ_2	0.47 ± 0.03	40.6 ± 1.8	1.5 ± 1.7
17V	γ_1	0.75 ± 0.03	58.2 ± 1.6	3.5 ± 2.6	17V	γ_1	0.76 ± 0.03	49.2 ± 1.9	0.1 ± 0.2
17V	γ_2	0.71 ± 0.03	68.2 ± 1.5	1.5 ± 1.6	17V	γ_2	0.72 ± 0.03	75.2 ± 1.6	0.0 ± 0.0
22T	γ_2	0.91 ± 0.03	29.8 ± 2.2	61.1 ± 10.5	22T	γ_2	0.95 ± 0.04	38.9 ± 2.6	52.9 ± 19.6
23V	γ_1	0.90 ± 0.04	53.4 ± 2.1	0.3 ± 0.5	23I	γ_2	0.76 ± 0.03	31.5 ± 1.8	1.1 ± 0.7
23V	γ_2	0.90 ± 0.04	77.0 ± 2.2	1.0 ± 1.4	23I	δ_1	0.47 ± 0.02	30.1 ± 1.0	0.4 ± 0.6
26F	—	—	—	—	26V	γ_1	n.d.	n.d.	2.1 ± 1.2
26F	—	—	—	—	26V	γ_2	0.74 ± 0.03	44.7 ± 1.9	0.3 ± 0.4
28A	β	0.86 ± 0.04	35.2 ± 1.7	59.7 ± 6.5	28A	β	0.74 ± 0.04	44.6 ± 2.1	57.3 ± 18.8
30I	γ_2	0.93 ± 0.04	40.6 ± 2.6	4.7 ± 4.3	30I	γ_2	0.88 ± 0.04	31.9 ± 2.0	0.4 ± 0.5
30I	δ_1	0.72 ± 0.03	10.3 ± 1.9	0.0 ± 0.0	30I	δ_1	0.65 ± 0.03	20.1 ± 1.7	1.0 ± 1.0
36I	γ_2	0.72 ± 0.03	92.9 ± 1.7	9.8 ± 6.3	36I	γ_2	0.71 ± 0.03	77.5 ± 1.9	11.5 ± 4.6
36I	δ_1	0.36 ± 0.02	31.4 ± 0.9	30.9 ± 12.7	36I	δ_1	0.48 ± 0.02	26.9 ± 1.0	23.6 ± 8.3
43L	δ_1	0.73 ± 0.05	72.8 ± 3.5	0.0 ± 0.1	43L	δ_1	0.47 ± 0.02	38.3 ± 1.3	0.6 ± 0.5
43L	δ_2	0.87 ± 0.07	63.2 ± 4.4	0.1 ± 0.2	43L	δ_2	n.d.	n.d.	0.7 ± 0.6
44I	γ_2	0.68 ± 0.03	35.7 ± 1.8	46.8 ± 11.6	44I	γ_2	0.60 ± 0.03	42.0 ± 1.5	28.1 ± 8.9
44I	δ_1	0.22 ± 0.01	31.5 ± 0.7	24.0 ± 23.6	44I	δ_1	0.16 ± 0.01	31.7 ± 0.8	37.7 ± 13.4
46A	β	0.89 ± 0.04	18.7 ± 2.2	61.5 ± 7.4	46A	β	0.83 ± 0.03	20.2 ± 2.2	46.9 ± 15.0
50L	δ_1	0.37 ± 0.02	71.2 ± 1.0	1.0 ± 1.7	50L	δ_1	0.66 ± 0.03	39.1 ± 2.2	0.0 ± 0.0
50L	δ_2	0.37 ± 0.02	44.9 ± 1.0	1.0 ± 1.5	50L	δ_2	0.70 ± 0.05	26.8 ± 2.7	1.1 ± 1.5
55T	γ_2	0.76 ± 0.03	39.5 ± 1.9	38.9 ± 7.2	55T	γ_2	0.85 ± 0.04	42.5 ± 2.0	36.0 ± 11.9
56L	δ_1	0.46 ± 0.02	81.1 ± 1.4	3.4 ± 2.1	56L	γ_1	0.60 ± 0.04	68.9 ± 2.8	0.0 ± 0.0
56L	δ_2	0.49 ± 0.02	39.3 ± 1.2	4.7 ± 3.5	56L	γ_2	0.62 ± 0.05	34.5 ± 2.9	0.3 ± 0.3
61I	γ_2	0.75 ± 0.03	28.9 ± 1.8	1.4 ± 1.4	61I	γ_2	0.69 ± 0.03	29.3 ± 1.6	0.0 ± 0.0
61I	δ_1	0.58 ± 0.02	15.9 ± 1.3	2.2 ± 1.9	61I	δ_1	0.54 ± 0.02	24.2 ± 1.3	0.0 ± 0.0
66T	γ_2	n.d.	n.d.	19.9 ± 6.6	66T	γ_2	n.d.	n.d.	12.3 ± 5.0
67I	γ_2	0.90 ± 0.04	46.4 ± 2.1	0.1 ± 0.2	67L	δ_1	0.24 ± 0.01	55.9 ± 0.8	0.0 ± 0.0
67I	δ_1	0.19 ± 0.01	19.8 ± 0.5	3.5 ± 3.0	67L	δ_2	0.21 ± 0.01	47.3 ± 0.7	1.4 ± 0.9
69L	δ_1	0.50 ± 0.02	42.0 ± 1.1	0.9 ± 1.0	69L	δ_1	n.d.	n.d.	0.0 ± 0.0
69L	δ_2	0.45 ± 0.02	44.5 ± 1.7	10.0 ± 4.6	69L	δ_2	n.d.	n.d.	9.0 ± 4.5
70V	γ_1	n.d.	n.d.	55.2 ± 16.6	70V	γ_1	n.d.	n.d.	39.0 ± 12.4
70V	γ_2	0.35 ± 0.01	71.6 ± 0.9	20.4 ± 5.3	70V	γ_2	0.34 ± 0.02	74.3 ± 1.1	39.9 ± 13.5
71L	δ_1	0.23 ± 0.01	50.4 ± 0.7	41.7 ± 23.9	71L	δ_1	0.22 ± 0.01	51.0 ± 0.6	68.4 ± 26.6
71L	δ_2	0.29 ± 0.02	46.8 ± 0.9	33.7 ± 24.6	71L	δ_2	n.d.	n.d.	8.0 ± 6.3
73L	δ_1	0.15 ± 0.02	43.2 ± 0.7	77.5 ± 20.0	73L	δ_1	0.13 ± 0.01	43.7 ± 0.5	72.5 ± 25.7
73L	δ_2	0.16 ± 0.01	39.3 ± 0.5	85.4 ± 12.9	73L	δ_2	0.14 ± 0.01	38.4 ± 0.4	74.6 ± 26.8

Solvent-accessible surface area is displayed as the percent solvent exposure of the methyl groups, calculated using the program MOLMOL (Koradi et al., 1996) with a probe radius of 1.4 Å. The values given are the average and standard deviation of the accessibilities of the ensemble of solution structures. Residues where motional parameters were not determined because of spectral overlap are indicated by 'n.d.'.

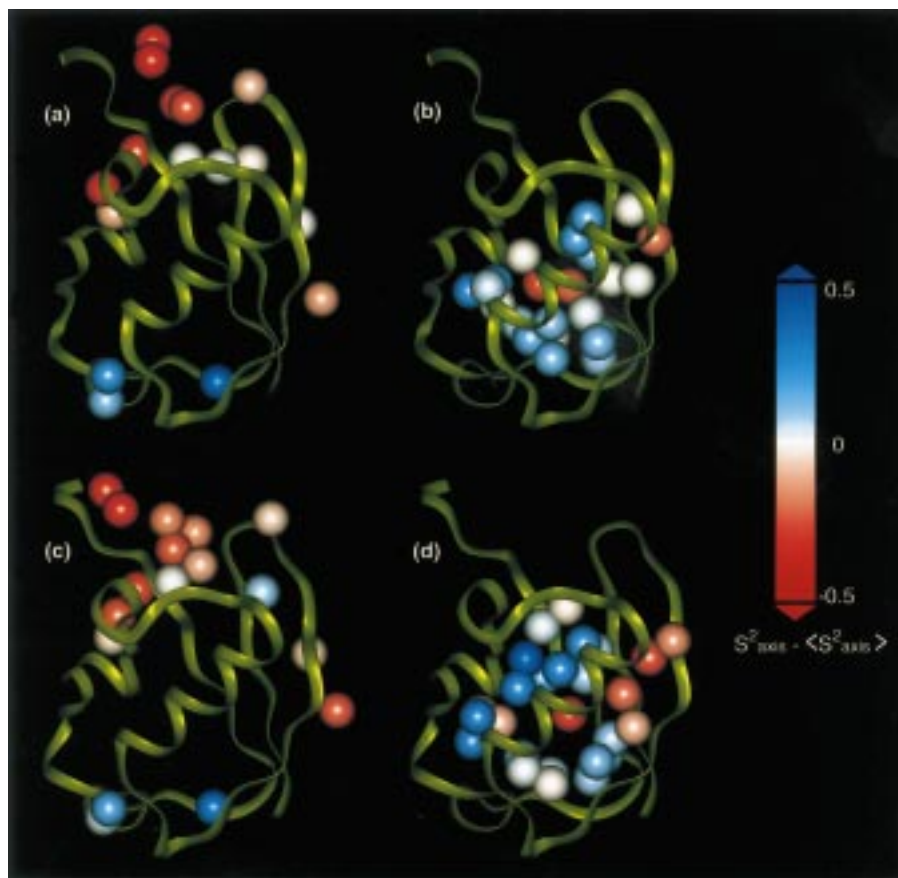


Figure 1. Methyl order parameters mapped onto the structures of WT (a and b), and 1D7 (c and d). Surface methyls are shown in (a) and (c), and core methyls are shown in (b) and (d). The color of the methyl corresponds to the difference between the measured order parameter and the average order parameter for that methyl type, as discussed in the text. Red methyls are more dynamic than average and blue methyls are less dynamic than average.

tions of these solvent-exposed methyls can easily be explained by the likely presence of these hydrogen bonds, as suggested by amide protection factors on the order of 10^4 in both proteins (Johnson et al., 1999).

Dynamics of core residues

A wide range of mobilities are present in the cores of both WT and 1D7 (Figures 1 and 3). Figure 4 shows the distribution of methyl order parameters, relative to the average, for both surface and core residues. Essentially the same range of mobilities is present in the core as is found for surface residues, although as mentioned above, the core is on average more ordered than the surface. Two core residues which have particularly low order parameters in both 1D7 and WT are residues 13 and 67. In WT, I13 has a much lower than average order parameter for its γ methyl ($S^2_{\text{axis}} = 0.51$), but an average order parameter for δ ($S^2_{\text{axis}} = 0.46$),

suggesting that there is a large amount of flexibility in the χ^1 rotamer, but not much additional motion about χ^2 . V13 in 1D7 has extremely low order parameters ($S^2_{\text{axis}} = 0.48, 0.38$), indicating that repacking the ubiquitin core did not affect the χ^1 flexibility for this residue. The flexibility of residue 13 could be due, in part, to its proximity with the slightly flexible loop between strands 1 and 2 (residues 10 and 11 in 1D7 and WT have backbone order parameters between 0.67 and 0.73, although the backbone at residue 13 is in fact well ordered ($S^2_{\text{NH}} = 0.85$ for 1D7; 0.84 for WT) (Johnson et al., 1999)). Additionally, this flexibility could be due to the greater solvent accessibility of residue 13 compared to other core residues (Table 1). Residue 67 is also highly dynamic in both proteins. I67 in 1D7 has a very rigid γ methyl ($S^2_{\text{axis}} = 0.90$) but a disordered δ ($S^2_{\text{axis}} = 0.19$), suggesting that the χ^1 angle is well defined while χ^2 undergoes large os-

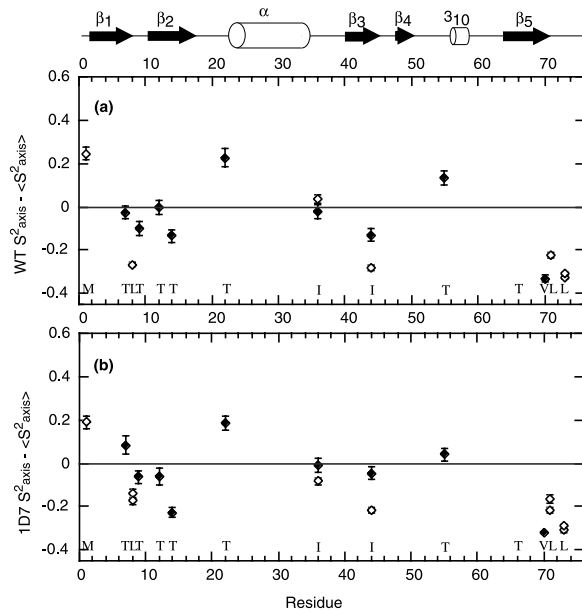


Figure 2. Plot of the difference of sidechain order parameters from average ($S^2_{\text{axis}} - \langle S^2_{\text{axis}} \rangle$) for surface residues of WT (a) and 1D7 (b). γ Methyls are displayed as open symbols, and δ and ϵ methyls are displayed as filled symbols.

cillations. In WT the corresponding residue, L67, has low order parameters ($S^2_{\text{axis}} = 0.24, 0.21$). These order parameters do not by themselves distinguish between the possibilities that the sidechain flexibility is the result of fluctuations about both χ^1 and χ^2 , or that χ^1 is rigid and the flexibility is due only to rotations about χ^2 . However, J-coupling data (Hu and Bax, 1997) suggests that L67 has a well-defined χ^1 , similar to I67 in 1D7. Interestingly, this dynamic behavior may be correlated with the fact that in both WT and 1D7, residue 67 populates a highly strained rotamer conformation due to an unfavorable χ^2 . We previously noted the tendency for such residues to sample statistically more favored rotamers (Johnson et al., 1999). Regardless of the reason, repacking the core of ubiquitin has not affected the dynamic behavior of these two residues, even though they were both mutated.

By contrast, a number of core sidechains, including mutated and non-mutated residues, do show differences in order parameters for 1D7 and WT. While L50 became more flexible in 1D7 (WT $S^2_{\text{axis}} = 0.66, 0.70$; 1D7 $S^2_{\text{axis}} = 0.37, 0.37$), L43 became more rigid (WT $S^2_{\text{axis}} = 0.47, \text{n.d.}$; 1D7 $S^2_{\text{axis}} = 0.73, 0.87$). In fact, L43 in 1D7 has the highest Leu order parameters of both proteins. Similarly, residue 23 became much more rigid in the 1D7 core. In WT, I23 has average

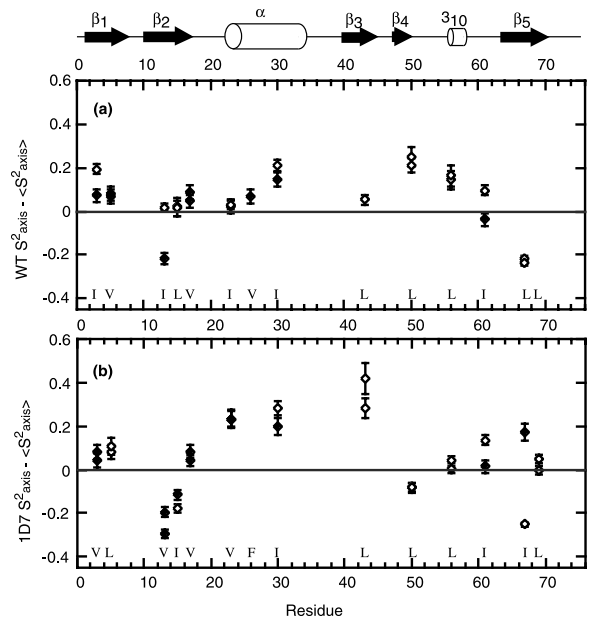


Figure 3. Plot of the difference of sidechain order parameters from average ($S^2_{\text{axis}} - \langle S^2_{\text{axis}} \rangle$) for core residues of WT (a) and 1D7 (b). γ Methyls are displayed as open symbols, and δ methyls are displayed as filled symbols.

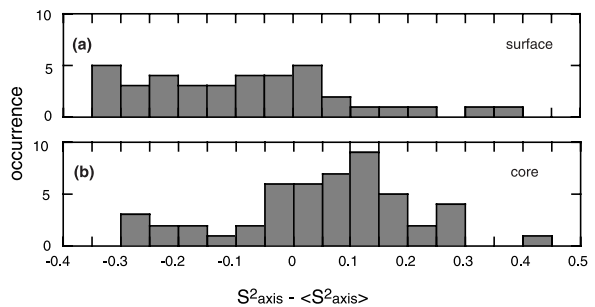


Figure 4. Distribution of 1D7 and WT order parameters, presented as $S^2_{\text{axis}} - \langle S^2_{\text{axis}} \rangle$, for (a) surface and (b) core residues.

order parameters ($S^2_{\text{axis}} = 0.76 \gamma, 0.47 \delta$), whereas in 1D7, V23 has the highest order parameters of any Val in either WT or 1D7 ($S^2_{\text{axis}} = 0.90, 0.90$). Finally, residue 15 becomes more flexible in 1D7. L15 in WT has average order parameters ($S^2_{\text{axis}} = 0.47, 0.47$), while I15 in 1D7 has low order parameters for both the γ and δ methyls ($S^2_{\text{axis}} = 0.62\gamma, 0.26\delta$). Thus, while we observe a number of changes in flexibility of specific sidechains in the cores of 1D7 and WT, the overall dynamic nature of the two proteins is fairly similar. Qualitatively, it seems that repacking has caused a redistribution of the dynamic behavior amongst different residues in the core. The redistribution is not correlated with changes in backbone flexibility since

Table 2. Three-bond coupling constants (in Hz) for 1D7

		$^3J_{\text{NC}\gamma}$	$^3J_{\text{COC}\gamma}$			$^3J_{\text{C}\delta\text{C}\alpha}$
V3	γ_1	0.6	3.9	L5	δ_1	3.7
V3	γ_2	0.6	1.4	L5	δ_2	n.d.
V13	γ_1	1.1	2.2	L8	δ_1	3.2
V13	γ_2	0.7	2.3	L8	δ_2	1.6
V17	γ_1	0.4	3.7	L43	δ_1	3.5
V17	γ_2	0.7	1.0	L43	δ_2	n.d.
V23	γ_1	2.3	1.1	L50	δ_1	2.7
V23	γ_2	0.4	4.1	L50	δ_2	2.5
V70	γ_1	n.d.	n.d.	L56	δ_1	2.9
V70	γ_2	0.5	2.6	L56	δ_2	2.1
				L69	δ_1	1.4
T7		1.1	2.7	L69	δ_2	3.7
T9		0.9	3.1	L71	δ_1	2.6
T12		1.6	0.7	L71	δ_2	2.2
T14		1.4	1.5	L73	δ_1	2.9
T22		0.8	3.5	L73	δ_2	1.8
T55		0.9	3.0			
T66		n.d.	n.d.	I15		n.d.
				I30		3.2
I15		1.7	0.7	I36		2.7
I30		2.3	1.0	I44		n.d.
I36		2.1	0.8	I61		3.2
I44		1.8	0.7	I67		1.6
I61		2.2	1.2			
I67		2.2	0.7			

Intermediate values of the three-bond coupling constants, which are indicative of conformational averaging, are shown in bold.

for the positions cited above, the NH order parameters are high and indistinguishable between 1D7 and WT (Johnson et al., 1999).

Consistency with structural data and coupling constant measurements

Our sidechain order parameters show good agreement with previously reported structural data. For 1D7, residues which have low sidechain order parameters have a spread in rotamers in the ensemble of solution structures. This is particularly notable in the core, where sidechains are generally defined by a larger number of NOE distance constraints. The four 1D7 core residues, which have lower than average methyl order parameters (residues 13, 15, 50, and 67), sample multiple rotamers in the ensemble of structures. Each of the remaining core residues populates only a single χ^1 rotamer or χ^1/χ^2 rotamer pair.

Our 1D7 sidechain dynamics are also corroborated by measurements of three-bond coupling constants be-

tween methyl carbons and backbone atoms (Table 2), which were used in our structure calculations to help define χ^1 and χ^2 angles. The values of $^3J_{\text{NC}\gamma}$ and $^3J_{\text{COC}\gamma}$ depend on the χ^1 angle of Val, Thr, and Ile residues, and the value of $^3J_{\text{C}\delta\text{C}\alpha}$ depends on the χ^2 angle of Ile and Leu residues. Large coupling constants (approximately greater than 2 Hz for $^3J_{\text{NC}\gamma}$ and greater than 3 Hz for $^3J_{\text{COC}\gamma}$ and $^3J_{\text{C}\delta\text{C}\alpha}$) are indicative of *trans* orientations, while small coupling constants (approximately less than 1 Hz for $^3J_{\text{NC}\gamma}$ and less than 1.5 Hz for $^3J_{\text{COC}\gamma}$ and $^3J_{\text{C}\delta\text{C}\alpha}$) are indicative of *gauche* orientations. Intermediate values are the result of either eclipsed rotamers or dynamic averaging of multiple rotamers. All residues which have intermediate values of the coupling constants (in bold in Table 2) have either average or below average methyl order parameters. For example, the intermediate values of $^3J_{\text{COC}\gamma}$ for V13 and $^3J_{\text{NC}\gamma}$ for I15 reflect the mobility of these residues about χ^1 . Similarly, the intermediate value of $^3J_{\text{C}\delta\text{C}\alpha}$ for L50 reflects its mobility about χ^2 .

The ensemble of solution structures for WT does not show a spread in sidechain rotamer populations to the same extent that the 1D7 structure does, suggesting a slightly higher degree of flexibility in 1D7. However, in the structure calculations of the WT protein (Cornilescu et al., 1998), a conformational energy term (Kuszewski et al., 1997) was included. This could potentially force an unconstrained sidechain into the statistically most favored rotamer when the sidechain is actually sampling multiple conformations, making the presence or absence of a spread in rotamers more difficult to interpret. Nevertheless, it is interesting to note that the two WT core residues with lower than average order parameters, I13 and L67, both have different sidechain conformations in the solution structure and the two crystal structures (Vijay-Kumar et al., 1987; Alexeev et al., 1994). These data illustrate that inconsistencies in structures can arise from dynamics rather than inaccuracies or a lack of precision in structure calculations.

Discussion

Our data do not show a clear tendency of dynamic sidechains to cluster together. The two surface residues with higher than average order parameters, T22 and T55, are packed against each other, suggesting that their restricted motions could be related. In the core, however, being packed against rigid residues does not necessarily result in restricted motion. In both

1D7 and WT, the δ methyls of residue 67 have low order parameters despite being surrounded by core residues with either average or above average order parameters. Additionally, the sidechains of residues 23 and 43 are adjacent, and the mutations in the core of 1D7 resulted in both of these sidechains becoming significantly more ordered than in WT. However, these residues are also packed against the sidechain of L50 which changed from well ordered in WT to highly mobile in 1D7.

Even though there is no obvious relationship between dynamics of neighboring residues, the core packing mutations in 1D7 do affect the dynamics of surrounding residues. L43 and L50 are not mutated in 1D7, yet they have significantly different order parameters than in WT. Overall, the level of methyl dynamics in the WT and 1D7 cores is fairly similar, especially for the surface residues. However, 1D7 does show a slightly greater tendency for sampling of multiple sidechain conformations in the core. In addition, there are differences in the location of the core residues which show dynamic behavior. One possible explanation for this is that sidechain dynamics may be partially the result of rotamer strain. We previously noted that sidechains in strained rotamer conformations, such as residue 67 in both WT and 1D7, tend to be more flexible. Similarly, dynamic residues 13 and 15 in 1D7 were predicted to be in statistically unfavorable rotamers, but in the ensemble of solution structures, these residues populate the most favored rotamers in addition to the predicted less favored conformations (Johnson et al., 1999). The mobility may reduce unfavorable steric interactions within the sidechain or between the sidechain and the backbone. At the same time, a loss in favorable interactions may be partially compensated by an increase in conformational entropy. Alternatively, the change in location of dynamic residues may be caused by a slight alteration in the spatial relationships of secondary structural elements. This could result in either the disruption or formation of stabilizing interactions that alter sidechain motion locally or distant from the site of mutation.

The differences in the dynamics of WT and 1D7 are subtle. However, this does not suggest that in general core packing has only a minimal effect on dynamics. Ubiquitin is inherently a well-ordered protein, and 1D7 is the most stable of our mutants designed to resemble WT ubiquitin by having a well-packed core. Elsewhere we describe the structure of a more destabilized ubiquitin variant (1D8) which also has

the same core volume as WT; compared to both WT and 1D7, this variant displays greater conformational flexibility in the backbone, as evident by the presence of conformational exchange peaks for backbone amide resonances, and in the core, as demonstrated by a greater spread in core sidechain rotamers (Lazar et al., *Protein Sci.*, in press). Furthermore, in the context of an intrinsically more flexible protein, larger dynamic changes are likely in response to packing.

Other studies have demonstrated the connection between packing, dynamics, and function. For example, an M190A core mutation in α -lytic protease altered the dynamics in the substrate pocket and relaxed the specificity of the enzyme (Miller and Agard, 1999). Similarly, an A77V mutation in the *trp* repressor decreased the flexibility of its binding domain, resulting in increased affinity for the *trp* operator, yet decreased affinity for the *aroH* and *trpR* operators (Gryk et al., 1996). Our data complement these studies by showing that packing can affect dynamics, even in a well-ordered protein where core volume is conserved. Clearly, for rational design or re-engineering of binding specificity and function, a deep and quantitative understanding of the factors that affect dynamics will be necessary.

Conclusions

The mutations in 1D7 affected the dynamics of a number of the methyl groups within the core, yet the overall dynamic nature of the protein remained largely the same. For as many sidechains that had increased mobility in the mutant, almost as many sidechains had decreased mobility. At the same time, the core mutations had little effect on the dynamics of sidechains on the surface of the protein. This confirms, at a fairly detailed level, the ability of our core repacking algorithm to redesign protein cores. The most interesting observation was that core packing in 1D7 caused a redistribution of the dynamic behavior and that this correlates with residues that have a tendency to populate unfavorable rotamer conformations. This suggests that dynamics may partially offset the effects of strain by reducing steric clash and increasing conformational entropy.

Acknowledgements

We would like to thank Susan Marqusee and Dave Wemmer for use of their NMR spectrometer for the

measurements at 500 MHz, John Marquardt and Ad Bax for providing the coordinates of the WT solution structure, and Julie Forman-Kay for providing the database of methyl order parameters. This work was supported by an NSF Young Investigator award to T.M.H.

References

- Akke, M., Skelton, N.J., Kordel, J., Palmer, A.G. and Chazin, W.J. (1993) *Biochemistry*, **32**, 9832–9844.
- Alexeev, D., Bury, S.M., Turner, M.A., Ogunjobi, O.M., Muir, T.W., Ramage, R. and Sawyer, L. (1994) *Biochem. J.*, **299**, 159–163.
- Bevington, P.R. (1969) *Data Reduction and Error Analysis for the Physical Sciences*, McGraw-Hill, New York, NY, pp. 119–127.
- Chatfield, D.C., Szabo, A. and Brooks, B.R. (1998) *J. Am. Chem. Soc.*, **120**, 5301–5311.
- Cheng, J.W., Lepre, C.A. and Moore, J.M. (1994) *Biochemistry*, **33**, 4093–4100.
- Constantine, K.L., Friedrichs, M.S., Wittekind, M., Jamil, H., Chu, C.H., Parker, R.A., Goldfarb, V., Mueller, L. and Farmer, B.T. (1998) *Biochemistry*, **37**, 7965–7980.
- Cornilescu, G., Marquardt, J.L., Ottiger, M. and Bax, A. (1998) *J. Am. Chem. Soc.*, **120**, 6836–6837.
- Dahiyat, B.I. and Mayo, S.L. (1996) *Protein Sci.*, **5**, 895–903.
- Dahiyat, B.I. and Mayo, S.L. (1997) *Science*, **278**, 82–87.
- Desjarlais, J.R. and Handel, T.M. (1995) *Protein Sci.*, **4**, 2006–2018.
- Faber, H.R. and Matthews, B.W. (1990) *Nature*, **348**, 263–266.
- Farrow, N.A., Muhandiram, R., Singer, A.U., Pascal, S.M., Kay, C.M., Gish, G., Shoelson, S.E., Pawson, T., Forman-Kay, J.D. and Kay, L.E. (1994) *Biochemistry*, **33**, 5984–6003.
- Gagne, S.M., Tsuda, S., Spyrapoulos, L., Kay, L.E. and Sykes, B.D. (1998) *J. Mol. Biol.*, **278**, 667–686.
- Gryk, M.R., Jardetzky, O., Klig, L.S. and Yanofsky, C. (1996) *Protein Sci.*, **5**, 1195–1197.
- Hecht, M.H., Richardson, J.S., Richardson, D.C. and Ogden, R.C. (1990) *Science*, **249**, 884–891.
- Hoch, J.C. and Stern, A.S. (1996) *NMR Data Processing*, Wiley-Liss, New York, NY, pp. 102–135.
- Hodsdon, M.E. and Cistola, D.P. (1997) *Biochemistry*, **36**, 2278–2290.
- Hu, J.S. and Bax, A. (1997) *J. Am. Chem. Soc.*, **119**, 6360–6368.
- Hurley, J.H., Baase, W.A. and Matthews, B.W. (1992) *J. Mol. Biol.*, **224**, 1143–1159.
- Johnson, E.C., Lazar, G.A., Desjarlais, J.R. and Handel, T.M. (1999) *Struct. Fold. Des.*, **7**, 967–976.
- Kamtekar, S., Schiffer, J.M., Xiong, H., Babik, J.M. and Hecht, M.H. (1993) *Science*, **262**, 1680–1685.
- Kay, L.E. (1998) *Biochem. Cell. Biol.*, **76**, 145–152.
- Kay, L.E., Muhandiram, D.R., Farrow, N.A., Aubin, Y. and Forman-Kay, J.D. (1996) *Biochemistry*, **35**, 361–368.
- Kay, L.E., Muhandiram, D.R., Wolf, G., Shoelson, S.E. and Forman-Kay, J.D. (1998) *Nat. Struct. Biol.*, **5**, 156–163.
- Kono, H., Nishiyama, M., Tanokura, M. and Doi, J. (1998) *Protein Eng.*, **11**, 47–52.
- Koradi, R., Billeter, M. and Wüthrich, K. (1996) *J. Mol. Graph.*, **14**, 51–55.
- Kuszewski, J., Gronenborn, A.M. and Clore, G.M. (1997) *J. Magn. Reson.*, **125**, 171–177.
- Lazar, G.A., Desjarlais, J.R. and Handel, T.M. (1997) *Protein Sci.*, **6**, 1167–1178.
- Lee, A.L., Flynn, P.F. and Wand, A.J. (1999) *J. Am. Chem. Soc.*, **121**, 2891–2902.
- Lienin, S.F., Bremi, T., Brutscher, B., Bruschweiler, R. and Ernst, R.R. (1998) *J. Am. Chem. Soc.*, **120**, 9870–9879.
- Lipari, G. and Szabo, A. (1982) *J. Am. Chem. Soc.*, **104**, 4546–4559.
- Malakauskas, S.M. and Mayo, S.L. (1998) *Nat. Struct. Biol.*, **5**, 470–475.
- Miller, D.W. and Agard, D.A. (1999) *J. Mol. Biol.*, **286**, 267–278.
- Mittermaier, A., Kay, L.E. and Forman-Kay, J.D. (1999) *J. Biomol. NMR*, **13**, 181–185.
- Olejniczak, E.T., Zhou, M.M. and Fesik, S.W. (1997) *Biochemistry*, **36**, 4118–4124.
- Palmer, A.G. (1997) *Curr. Opin. Struct. Biol.*, **7**, 732–737.
- Pinto, A.L., Hellinga, H.W. and Caradonna, J.P. (1997) *Proc. Natl. Acad. Sci. USA*, **94**, 5562–5567.
- Quinn, T.P., Tweedy, N.B., Williams, R.W., Richardson, J.S. and Richardson, D.C. (1994) *Proc. Natl. Acad. Sci. USA*, **91**, 8747–8751.
- Rader, S.D. and Agard, D.A. (1997) *Protein Sci.*, **6**, 1375–1386.
- Stivers, J.T., Abeygunawardana, C. and Mildvan, A.S. (1996) *Biochemistry*, **35**, 16036–16047.
- Vijay-Kumar, S., Bugg, C.E. and Cook, W.J. (1987) *J. Mol. Biol.*, **194**, 531–544.
- Wand, A.J., Urbauer, J.L., McEvoy, R.P. and Bieber, R.J. (1996) *Biochemistry*, **35**, 6116–6125.
- Wisz, M.S., Garrett, C.Z. and Hellinga, H.W. (1998) *Biochemistry*, **37**, 8269–8277.
- Wong, K.B. and Daggett, V. (1998) *Biochemistry*, **37**, 11182–11192.
- Yan, Y. and Erickson, B. (1994) *Protein Sci.*, **3**, 1069–1073.
- Yang, D., Mittermaier, A., Mok, Y.K. and Kay, L.E. (1998) *J. Mol. Biol.*, **276**, 939–954.
- Zanotti, G., Berni, R. and Monaco, H.L. (1993) *J. Biol. Chem.*, **268**, 10728–10738.